05,12

Topological bands in metals with helical magnetic order

© Yu.B. Kudasov

Sarov Institute of Physics and Technology, National Research Nuclear University „MEPhI“,
Sarov, Russia
Russian Federal Nuclear Center, All-Russia Research Institute of Experimental Physics,
Sarov, Russia

E-mail: yu_kudasov@yahoo.com

Received April 17, 2023
Revised April 17, 2023
Accepted May 11, 2023

The effect of a helicoidal magnetic field on the dispersion of conduction electrons in one- and two-dimensional systems is investigated. In a helicoidal periodic magnetic field, there is a special symmetry with respect to the reversal of time, which leads to the peculiarities of the band structure. Using an example of a one-dimensional model system, the topological properties of the band structure in an effective magnetic field corresponding to the 120°-ordering are investigated. In $PdCrO_2$, the 120° magnetic ordering of the dielectric layers of CrO_2 creates an unusual spin structure of the Fermi surface in conducting palladium layers. In this case, the umklapp scattering of mobile charge carriers is strongly suppressed, which leads to abnormally high conductivity at low temperatures observed experimentally.

Keywords: Helicoidal ordering, Time-reversal symmetry, Band structure, Charge carriers scattering, Metallic delafossites, $PdCrO_3$.

DOI: 10.21883/PSS.2023.06.56098.04H

1. Introduction

Delafossites — are compounds with the general formula ABO_2, having a layered structure with alternating hexagonal ion layers A and BO_2. These 3d-metal-based compounds ($B = \mathrm{Cr, Fe, Co}$) exhibit a variety of magnetic and transport properties that have attracted the attention of theorists and experimentalists. Thus, the geometric frustration in $CuFeO_2$ leads to several types of magnetic ordering which alternate in the magnetic field [1], and partial substitution of ions Fe^{3+} by Al^{3+} leads to multiferroic behavior [2]. The compounds $PdCoO_2$, $PtCoO_2$, $PdCrO_2$ etc. form the metallic delaphossite group. The electrical conductivity of these substances is a record for metallic oxides and appears to be comparable to values typical of elemental metals such as copper and silver [3]. The CoO_2 and CrO_2 layers are dielectric, and the conductivity is only provided by platinum or palladium [4,5] layers, resulting in anomalous free path lengths. For example, in $PdCoO_2$ at room temperature, it is 700 Å and at low temperatures, it reaches 20 μm [3]. This suggests an unusual mechanism of electron transport in metallic delaphossites; in particular, a transition to a hydrodynamic mode of motion of conduction electrons [6] was observed in them. The mechanism responsible for the anomalous transport properties of these compounds [7] has recently been actively sought.

Among metallic delaphossites with anomalous conductivity, $PdCrO_2$ — the only compound in which a long-range magnetic order ($T_N = 38$ K) [8] occurs. The magnetic structure turns out to be extremely complex: chromium ions in CrO_2 dielectric interlayers form an 120°-ordering with alternating chirality in neighboring interlayers. In total, the magnetic structure consists of 18 sublattices [9]. The transition to a magnetically-ordered state leads to a sharp drop in resistance. It should be noted, that $PdCrO_2$ is an extremely rare example of a compound exhibiting an unconventional anomalous Hall effect at zero total chirality [10]. Magnetothermode studies have shown that the near magnetic order in $PdCrO_2$ is conserved up to room temperature and above [11].

The motion of a particle of spin 1/2 in a helicoidal magnetic field has been studied for quite a long time [12–17]. Particularly, the exact solution of the one-dimensional problem for a homogeneous helicoidal field [12] is known. Nowadays, interest in helimagnetics has been revived by the discovery of electron transport [15] and the possibility of current control of magnetic structure [16] therein. An overview of the current state of theoretical and experimental studies of uniaxial helimagnetics is presented in [17]. In the present paper, we study the electronic structure in a helicoidal magnetic field from symmetric and topological points of view.

2. Theoretical background

Consider a crystal lattice described by symmetry operations $\{\alpha_{\mathbf{R}}|\mathbf{t}\}$: $\alpha_{\mathbf{R}}$ — rotate around axis $\mathbf{R}$ by angle α and translate to vector $\mathbf{t}$. Suppose that there is also a helicoidal ordering of spins in the crystal. Let us assume that the spins lie in the same plane, and in the absence of spin-orbit coupling, the spin plane choice is arbitrary, i.e., it does not affect the dispersion curves of the electrons. Let us also assume that when translating to vector $\mathbf{t}$, the spins

are rotated by angle $\alpha_S(t)$, and the magnetic structure is commensurable, that is, the translation vector of magnetic structure $\mathbf{T}_m$ is a multiple of vector $\mathbf{t}$. The symmetry of such a helicoidal structure can be described by a spin space group with elements $\{\alpha_S|\alpha_\mathbf{R}|\mathbf{t}\}$ [18,19]. Thus, along the helicoid direction, we have two multiple periods of translation. For translation T_m, Bloch's theorem holds, and for the combined $\{\alpha_\mathbf{R}|\mathbf{t}\}$ operation, the generalized Bloch's theorem [19] holds. As we shall see below, this leads to non-trivial consequences for the topological structure of conduction bands. Note, that in [12], we found a kind of operator similar to the momentum operator commuting to the Hamiltonian and determining the quantum numbers of the spectrum branches in the helicoidal field. Note, however, that this approach is only possible for a homogeneous helicoid where a continuous symmetry transformation (translation with rotation) exists. The spin space group approach seems more suitable for the study of real systems.

Topological properties of the [20] zone structure have been extensively studied in the last decades. The appearance of topological properties of the band structure of crystalline substances is related to the presence of periodic boundary conditions at the borders of the Brillouin zone. Thus, for a one-dimensional system, the points with wave vectors $\mathbf{k} = \pi$ and $\mathbf{k} = -\pi$ are equivalent, i.e. the dispersion curves correspond to closed lines on the cylinder. For two-dimensional systems, periodic boundary conditions similarly lead to dispersion surfaces on a torus [21]. The main focus is on studies of topological insulators and on edge states in these systems [20].

3. Time reversal symmetry and zone structure topology in helicoidal magnetic field

The equation of motion of free electrons in a helicoidal magnetic field has unusual properties with respect to the time reversal operation. Let us write the Hamiltonian for a particle (electron) of spin 1/2 moving in a scalar periodic potential V and a periodic magnetic field $\mathbf{h}(\mathbf{r})$ in the form

$$H = \frac{1}{2m}(\hat{\mathbf{p}} - e\mathbf{A})2 + V(\mathbf{r}) - \mathbf{h}(\mathbf{r})\hat{\boldsymbol{\sigma}}, \qquad (1)$$

where $\hat{\mathbf{p}}$ — momentum operator, $\hat{\boldsymbol{\sigma}}$ — Pauli matrices, $\mathbf{h}$ and $\mathbf{A}$ — magnetic field induction and vector potential ($\mathbf{h} = \mathrm{rot}\,\mathbf{A}$v). The magnetic field period is $\mathbf{a}_m$m, i.e.

$$\mathbf{h}(\mathbf{r} + \mathbf{a}_m) = \mathbf{h}(\mathbf{r}), \qquad (2)$$

and the potential $V(\mathbf{r})$ is translationally invariant with respect to the period shift $\mathbf{a}_m/2$. An example of a periodic magnetic field is a helicoid oriented along the axis z. The distribution of the magnetic field can be represented as

$$h_x = h_0\cos(Kz), \quad h_y = h_0\cos(Kz), \qquad (3)$$

where h_0 and $K = 2\pi/a_m$ — constants. For a periodic magnetic field $\mathbf{h}(\mathbf{r})$, it is always possible to select the vector potential also as a periodic function.

The general approach to the study of symmetry with respect to the time reversal operation in the magnetic field is to combine the time reversal operators $\hat{\theta}$ and some operation reversing the magnetic field direction [22]. In a homogeneous magnetic field oriented along axis z, the system is symmetric with respect to a combination of $\hat{\theta}$ reflection in a plane transmitting z axis or rotation on 180° around an axis perpendicular to z axis [3]. For a periodic helicoidal field (2) and (3), the only operation leading to $\mathbf{h} \to -\mathbf{h}$, apart from rotation about the axis z, is the translation along the axis z by half a helix period ($\hat{T}_{1/2}$). Thus, the combined operator $\hat{\theta}\hat{T}_{1/2}\hat{\theta}$ is a symmetry transformation. This, in turn, should lead to the condition [23]:

$$\varepsilon_{\mathbf{k},\langle\sigma\rangle} = \varepsilon_{-\mathbf{k},-\langle\sigma\rangle}, \qquad (4)$$

where $\varepsilon_{\mathbf{k},\langle\sigma\rangle}$ — energy of a particle with wave vector $\mathbf{k}$ and mean value of spin $\langle\sigma\rangle$. It should be noted that in a noncollinear structure, spin is generally not a good quantum number, so the state is characterized by its average value.

4. Tight binding approximation for one-dimensional chain

The simplest example of a helicoidal magnetic structure is a one-dimensional chain of identical atoms, in which the magnetic field, acting on the particle, is rotated by 120° in some plane in translation by one period of the chain. When there is no spin-orbit interaction, the plane, where the magnetic field lies, can be chosen arbitrarily, and in further we assume that this — plane xy. Such a chain has 3 sublattices and in the strong coupling approximation, can be described by the following Hamiltonian:

$$H = -\sum_{i,\sigma}(a_i^+ b_{i\sigma} + b_{i\sigma}^+ c_{i\sigma} + c_{i\sigma}^+ a_{i+1\sigma} + \mathrm{H.c.}) + \sum_i(\hat{\mathbf{h}}_{ia} + \hat{\mathbf{h}}_{ib} + \hat{\mathbf{h}}_{ic}), \qquad (5)$$

where $a_{i\sigma}^+$, $b_{i\sigma}^+$, $c_{i\sigma}^+$ — electron spin birth operators σ on sublattices a, b and c, $\hat{\mathbf{h}}_{a(b,c)}$ — operators of the form $\hat{\mathbf{h}}\mathbf{h}_{ia} = \sum \mathbf{h}_a a_{i\alpha}^+ \boldsymbol{\sigma}_{\alpha\beta} a_{i\beta}$. Here, $\mathbf{h}_{a(b,c)}$ — magnetic field on sublattices, $\boldsymbol{\sigma}_{\alpha\beta}$ — Pauli matrices, α, β — spin indices, H.c. — Hermitian conjugation.

The Hamiltonian (5) can be diagonalized exactly. The resulting dispersion curves are shown in Fig. 1 for the case $|\mathbf{h}_{a(b,c)}| = 0.2$. It can be seen that within the Brillouin magnetic zone (from $-\pi$ to π), they are not individually periodic. The dispersion curve is chosen so that the state changes continuously within the Brillouin zone. However, in general, the structure of 3 zones appears to be periodic, i.e. Bloch's theorem holds, but the zone numbers are rearranged when the zone structure is shifted by the inverse lattice vector.

According to the generalized Bloch's theorem [19], the smallest reduced translation is determined by the vector $\mathbf{t}$

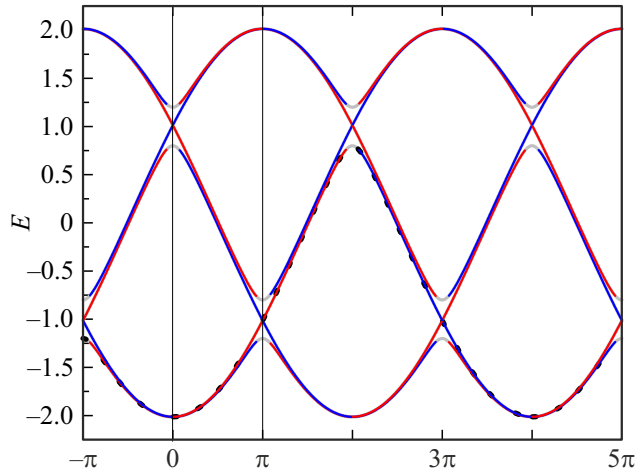

Figure 1. Dispersion curves for model (1) in the magnetic (from $-\pi$ to π) and extended Brillouin zones. Blue and red show predominantly spin up and spin down states ($\langle S\rangle \approx \pm 1/2$), respectively. Grey shows areas where there is strong mixing of spin states ($\langle S\rangle \approx \pm 1/4$). The dots show the dispersion curve within the extended Brillouin zone.

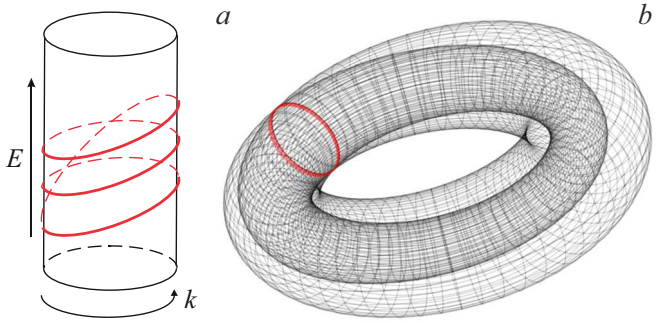

Figure 2. Schematic representation: a — dispersion curve for a one-dimensional model on a cylinder, b — an example of a dispersion surface on a torus (2D model) with self-intersection.

(with rotation of the spin system by the angle α_S). Then, we can construct a reduced magnetic lattice cell (as opposed to the usual magnetic cell corresponding to translation $\mathbf{T}_m$) and the corresponding extended Brillouin zone [5], which in this case coincides with the crystallochemical one. Within the extended magnetic Brillouin zone, the dispersion curves are periodic (marked by dots in Fig. 1). Thus, we get two periods for the zone structure. The result is illustrated in Fig. 2, *a*. If the magnetic Brillouin zone is represented on a cylindrical surface, the dispersion curve makes three revolutions, which corresponds to the period of the extended Brillouin zone.

In the energy area in Fig. 1 from -1.4 to -0.6, the branches symmetric with respect to the G-point have the opposite value of mean spin. In the approximation of almost free electrons in the one-dimensional case, similar solutions [23] are obtained.

5. 2D model of metallic hexagonal layer in $PdCrO_2$

In $PdCrO_2$, conductivity is determined by two-dimensional hexagonal palladium layers and 120°-th magnetic ordering in CrO_2 interlayers creates an effective field with a helicoidal structure. Set the model 2D distribution of the effective magnetic field as follows:

$$h_x(\mathbf{r}) = h_0\Big[\cos(\mathbf{K}_1\mathbf{r}) + \sin(\mathbf{K}_2\mathbf{r}) + \cos(K_3\mathbf{r})\Big],$$

$$h_y(\mathbf{r}) = h_0\Big[\sin(\mathbf{K}_1\mathbf{r}) + \cos(\mathbf{K}_2\mathbf{r}) + \sin(K_3\mathbf{r})\Big], \qquad (6)$$

where $\mathbf{K}_i$ — inverse lattice vector, $\mathbf{r}$ — forward lattice radius vector. The distribution (6) is shown in Fig. 3. You can clearly see that it has an 120°-th structure. It can be shown that the calculation results in the nearly free electron approximation do not depend qualitatively on the particular form of the potential, but are determined by its symmetry [23]. The system of equations describing the band structure in the nearly free electron approximation can be represented as [24]:

$$[E - (\mathbf{k} - \mathbf{K}_i)^2]c_{\mathbf{k}-\mathbf{K}_i,\alpha} = \sum_{j=1}^{m} \hat{U}_{\mathbf{K}_j-\mathbf{K}_i,\alpha\beta} c_{\mathbf{k}-\mathbf{K}_i,\beta}, \qquad (7)$$

where $c_{\mathbf{k}-\mathbf{K}_i,\beta}$ — the coefficient in the expansion of the Bloch's function. Unlike the expression in [24], the spin indices α, β are additionally introduced here, and the Fourier components of the potential $\hat{U}_{\mathbf{K}_i,\alpha\beta}$ contain non-diagonal spin components. The minimal 2D model to describe the hexagonal layer must contain two summation

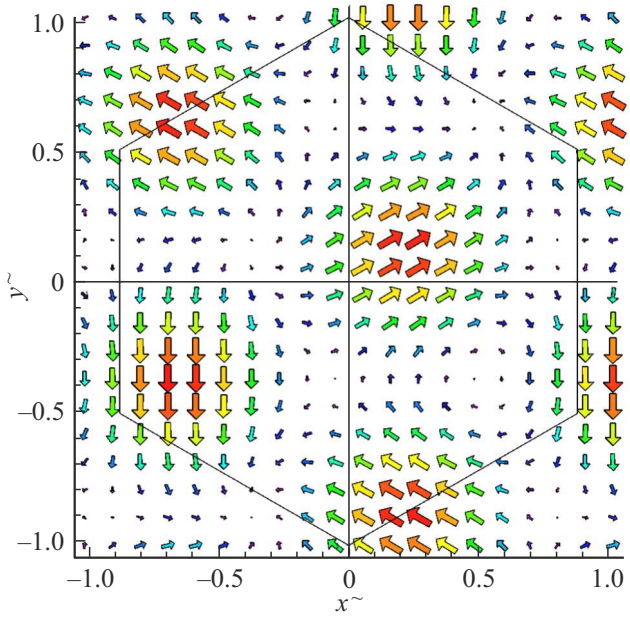

Figure 3. Model effective magnetic field distribution (6) corresponding to 120°-ordering.

terms (7), since the hexagonal Brillouin zone corners have to account for the terms for the two Bragg planes.

In paper [23], it is shown that in the case of a helicoidal magnetic field, the operators

$$\hat{U}_{\mathbf{K}} = \frac{1}{v}\int\limits_{Bz} \exp(-i\mathbf{K}\mathbf{r})\hat{h}(\mathbf{r})d\mathbf{r} \qquad (8)$$

are not normal, i. e. $\hat{U}_{\mathbf{K}}\hat{U}^{+}_{\mathbf{K}} \neq \hat{U}^{+}_{\mathbf{K}}\hat{U}_{\mathbf{K}}$ or $\hat{U}_{\mathbf{K}}\hat{U}_{-\mathbf{K}} \neq \hat{U}_{-\mathbf{K}}\hat{U}_{\mathbf{K}}$. Here, the integration is performed over the Brillouin zone. This leads to a dispersion relation of the form (4).

The results of calculating the band structure of the hexagonal layer in the approximation of almost free electrons with effective field (6) at $h_0 = 2$ are shown in Fig. 4. If the Fermi level falls in the area of energies between *1* and *2* lines, a large γ- orbit and „pockets“ in the K-point area form, as observed in $PdCrO_2$ below Curie temperature [25]. In the case where it falls in the area between the *1* and *2* lines, only a large γ- orbit is formed (see Fig. 5). It alternates between areas with predominantly opposite spinal directions.

The electronic structure of the 2D model has similar features to the one-dimensional model discussed above. Within a Brillouin magnetic zone, it is not the dispersion surfaces alone that are periodic, but the zone structure as a whole. The dispersion curves are periodic in the extended magnetic Brillouin zone. When the dispersion surfaces are depicted on a torus (periodic conditions for a 2D lattice), they appear to be self-intersecting. While for the one-dimensional chain, the intersections were at points (Fig. 2, *a*), for the 2D system, the intersections generally occur along lines. An example of a self-intersecting surface on a torus is shown in Fig. 2, *b*.

6. Properties of transport properties in $PdCrO_2$

In paper [23], the transport properties of one and two-dimensional systems in a helicoidal magnetic field have been qualitatively discussed. For the chain in Fig. 1, one can see that when the Fermi level falls in the energy range from -1.4 to -0.6, the transport properties are unusual. Here, only two branches with opposite spins cross the Fermi level. Therefore, an undamped spin current can occur. In order to describe this phenomenon correctly, the boundaries of the sample must be taken into account. Secondly, scattering backwards without a back flip is forbidden. This is much like the properties of edge states in topological insulators [20]. It should be noted that these properties are rather general, since they do not depend on the model used: in [21] the 1D approximation of almost free electrons was used, while in the present paper — the strong bond approximation.

Fig. 5 shows the Fermi surface calculated with the same parameters as for Fig. 4, for the case of the Fermi level lying between the lines *1* and *2* in Fig. 4. In this case, there is only an γ- Fermi surface orbit. At low temperatures, the phonon component of the electrical resistance is determined

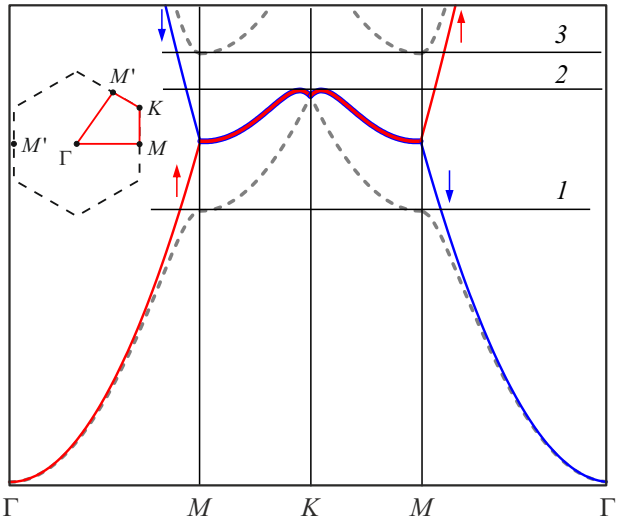

Figure 4. Calculated zone structure of the 2D model along the path shown in color in the insert.

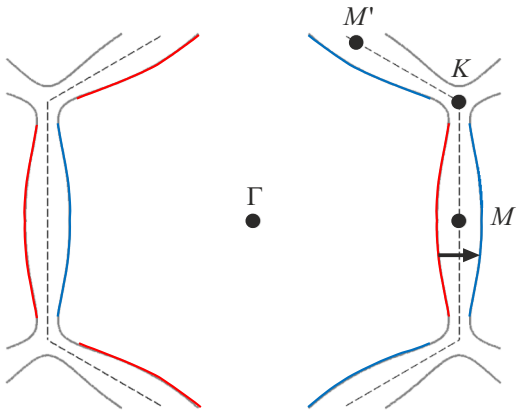

Figure 5. The Fermi surface for the case where the Fermi level falls between the levels *1* and *2* in Fig. 4. The color shows spin states with predominantly opposite directions. The grey line shows where there is strong mixing of spin states ($\langle S\rangle < 1/4$).

by overshooting processes [26]. However, overshooting by phonon scattering of electrons on adjacent arcs, as shown by the arrow in Fig. 5, is forbidden, as the initial and final states have opposite spins. This prohibition is not complete, since near the corners (point K), there is mixing of spin states (marked in grey), and in these areas the overshuffling processes are allowed. However, as shown in [23], the phonon resistance can decrease by about an order of magnitude for $PdCrO_2$. Scattering on non-magnetic impurities must also be partly suppressed by a partial backward scattering ban, again due to opposite electron initial and final state spins.

7. Conclusion

It is shown, that the zones in the helicoidal system are topologically nontrivial. An example of a two-dimensional

system with almost free electrons is the palladium planes in $PdCrO_2$, which are subject to 120°-effective field created by the chromium ions in the CrO_2 interlayers. The remaining metallic delafossites ($PdCoO_2$, $PtCoO_2$), although lacking long-range magnetic order, show signs of a strong short-range magnetic order over a wide temperature range [27]. The proposed mechanism of high conductivity can therefore be extended to these compounds as well.

Funding

This paper was supported by the National Centre for Physics and Mathematics (Direction No. 7 „Research in Strong and Superstrong Magnetic Fields“).

Conflict of interest

The author declares that he has no conflict of interest.

References

[1] T.T.A. Lummen, C. Strohm, H. Rakoto, P.H.M. Loosdrecht. Phys. Rev. B **81**, *22*, 224420 (2010).
[2] T. Arima. J. Phys. Soc. Jpn. **76**, *7*, 073702 (2007).
[3] A.P. Mackenzie. Rep. Prog. Phys. **80**, *3*, 032501 (2017).
[4] V. Eyert, R. Fresard, A. Maignan. Chem. Mater. **20**, *6*, 2370 (2008).
[5] F. Lechermann. Phys. Rev. Mater. **2**, *8*, 085004 (2018).
[6] T. Scaffidi, N. Nandi, B. Schmidt, A.P. Mackenzie, J.E. Moore. Phys. Rev. Lett. **118**, *22*, 226601 (2017).
[7] H. Usui, M. Ochi, S. Kitamura, T. Oka, D. Ogura, H. Rosner, M.W. Haverkort, V. Sunko, P.D.C. King, A.P. Mackenzie, K. Kuroki. Phys. Rev. Mater. **3**, *4*, 045002 (2019).
[8] K.P. Ong, J. Zhang, J.S. Tse, P. Wu. Phys. Rev. B **81**, *11*, 115120 (2010).
[9] H. Takatsu, G. Nenert, H. Kadowaki, H. Yoshizawa, M. Enderle, S. Yonezawa, Y. Maeno, J. Kim, N. Tsuji, M. Takata, Y. Zhao, M. Green, C. Broholm. Phys. Rev. B **89**, *10*, 104408 (2014).
[10] H. Takatsu, S. Yonezawa, S. Fujimoto, Y. Maeno. Phys. Rev. Lett. **105**, *13*, 137201 (2010).
[11] S. Arsenijevic, J.M. Ok, P. Robinson, S. Ghannadzadeh, M.I. Katsnelson, J.S. Kim, N.E. Hussey. Phys. Rev. Lett. **116**, *8*, 087202 (2016).
[12] M. Calvo. Phys. Rev. B **18**, *9*, 5073 (1978).
[13] M. Calvo. Phys. Rev. B **19**, *11*, 5507 (1979).
[14] E.L. Nagaev. Fizika magnitnykh poluprovodnikov. Nauka, M., (1979). (in Russian).
[15] H. Watanabe, K. Hoshi, J. Ohe. Phys. Rev. B **94**, *12*, 125143 (2016).
[16] N. Jiang, Y. Nii, H. Arisawa, E. Saitoh, Y. Onose. Nature Commun. **11**, 1601 (2020).
[17] J. Kishine, A.S. Ovchinnikov. Theory of Monoaxial Chiral Helimagnet. In: Solid State Physics. Book ser. (2015). V. 66. P. 1.
[18] W. Brinkman, R.J. Elliott. Proc. Roy. Soc. A **294**, *1438*, 343 (1966).
[19] L.M. Sandratskii. Phys. Status Solidi B **135**, *1*, 167 (1986).
[20] M.Z. Hasan, C.L. Kane. Rev. Mod. Phys. **82**, *4*, 3045 (2010).
[21] J. Cayssol, J.N. Fuchs. J. Phys. Mater. **4**, *3*, 034007 (2021).
[22] E. P. Wigner, Group Theory and its Application to the Quantum Mechanics of Atomic Spectra, (Academic Press Inc., New York, 1959) IL, M. (1961). (in Russian).
[23] Yu.B. Kudasov, JETP Lett. **113**, *3*, 155 (2021).
[24] N.W. Ashcroft, N.D. Mermin. Solid State Physics. Cengage Learning (1976).
[25] C.W. Hicks, A.S. Gibbs, A.P. Mackenzie, H. Takatsu, Y. Maeno, E.A. Yelland. Phys. Rev. Lett. **109**, *11*, 116401 (2012).
[26] J.M. Ziman. Electrons and Phonons. Clarendon Press (1960).
[27] T. Harada, K. Sugawara, K. Fujiwara, M. Kitamura, S. Ito, T. Nojima, K. Horiba, H. Kumigashira, T. Takahashi, T. Sato, A. Tsukazaki. Phys. Rev. Res. **2**, *1*, 013282 (2020).

Translated by Ego Translating